

Is TrueFISP a Gradient-Echo or a Spin-Echo Sequence?

Klaus Scheffler* and Jürgen Hennig

It is commonly accepted that TrueFISP (balanced FFE, FIESTA) belongs to the class of gradient-echo (GRE) sequences. GRE sequences are sensitive to dephasing effects of the transverse magnetization between the excitation pulse and echo acquisition, and phase coherence is only established directly after and before excitation pulses. However, an analysis of the phase evolution of transverse magnetization in a TrueFISP experiment shows very close similarities to the echo formation of a spin-echo (SE) experiment. If dephasing between excitation pulses is below $\pm\pi$, TrueFISP exhibits a nearly complete refocusing of transverse magnetization at $TE = TR/2$. Only signals acquired before and after $TR/2$ show an additional T_2^* sensitivity. Magn Reson Med 49:395–397, 2003. © 2003 Wiley-Liss, Inc.

Key words: steady-state free precession; refocusing; phase coherence; susceptibility

The signal intensity for steady-state GRE sequences depends on the chosen refocusing scheme. The RF-spoiled fast low-angle shot (FLASH) sequence exhibits a mainly T_1 -weighted contrast, whereas refocused GRE sequences (balanced along the phase-encoding direction, and not balanced along the slice-select and read directions) show an additional T_2 dependence due to partially refocused magnetization. The completely balanced TrueFISP sequence (balanced FFE, FIESTA) (1) shows an even stronger T_2 contribution, as given by

$$S_{TF} = M_0 \frac{(1 - E_1) \sin \alpha}{1 - (E_1 - E_2) \cos \alpha - E_1 E_2} \quad [1]$$

where $E_{1,2} = e^{-TR/T_{1,2}}$, and α is the flip angle (2). These formulas are only valid if the magnetization is measured directly after the preceding excitation pulse. For most applications a certain echo time (TE) is required to read out the GRE. It is thus commonly accepted that the measured signal at TE is additionally reduced by a factor of e^{-TE/T_2^*} , which accounts for dephasing effects during the time period between excitation and echo refocusing. This additional T_2^* dependence cannot be observed in SE sequences.

In the present work we analyze in more detail the T_2^* sensitivity of the TrueFISP sequence. It can be demonstrated that the phase evolution of the magnetization between two excitation pulses of a TrueFISP sequence is very similar to an SE or Carr-Purcell-Meiboom-Gill (CPMG) sequence, showing a nearly complete refocusing at $TE = TR/2$ and a T_2^* -related dephasing before and after

$TR/2$. Therefore, if TE is chosen to be exactly at $TR/2$, there is no additional signal weighting with e^{-TE/T_2^*} , as with other GRE sequences. The formula given in Eq. [1] thus has to be multiplied with e^{-TE/T_2} (if $TE = TR/2$) rather than with e^{-TE/T_2^*} .

THEORY

Neglecting diffusion effects, the transverse magnetization of a steady-state free precession (SSFP) experiment after the excitation pulse is given by (3)

$$M_y^+(\theta) = M_0 (1 - E_1)((1 - E_2 \cos \theta) \sin \alpha) / D \quad [2]$$

$$M_x^+(\theta) = M_0 (1 - E_1)(E_2 \sin \alpha \sin \theta) / D \quad [3]$$

with

$$D = (1 - E_1 \cos \alpha)(1 - E_2 \cos \theta) - (E_1 - \cos \alpha)(E_2 - \cos \theta)E_2. \quad [4]$$

where θ is the phase evolution between excitation pulses separated by TR, and α is the flip angle of the excitation pulse with phase zero (rotation around the x-axis). For TrueFISP the dephasing θ between RF pulses should be small to avoid banding artifacts. The measured signal intensity $M_T(TE)$ at the TE after the excitation pulse is then given by

$$M_T(TE) = e^{-TE/T_2} \left| \int_V p(\theta) (M_x^+(\theta) + iM_y^+(\theta)) e^{i\theta TE/TR} d\theta \right| \quad 0 < TE < TR. \quad [5]$$

$p(\theta)$, is a distribution of different dephasing angles, and is given by the field distribution within the imaging volume V . The integral represents a complex summation over all magnetization vectors within the imaging volume, and $e^{i\theta TE/TR}$ is the dephasing of the magnetization between excitation pulse and TE.

SIMULATIONS AND EXPERIMENTS

The simulated amplitude and phase profile at $TE = TR/2$ is shown in Fig. 1. For $TE = TR/2$ the signal has zero phase for off-resonance frequencies ranging between $\pm 1/(2TR)$, which is similar to the formation of an SE. The phase evolution between two excitation pulses ($TE = 0 \dots TR$) is plotted in Fig. 2a for dephasing angles between $\pm\pi$ within one TR interval. For the used simulation parameters ($T_1 = 20 TR$, $T_2 = 15 TR$, $\alpha = 70^\circ$) the magnetization is refocused not exactly at $TE = TR/2$, but, depending on T_1 and T_2 , slightly before $TR/2$. For the limited range of dephasing angles between $\pm 0.8\pi$ the phase trajectories are compara-

Section of Medical Physics, Department of Diagnostic Radiology, University of Freiburg, Freiburg, Germany.

*Correspondence to: Klaus Scheffler, Ph.D., University of Basel, Dept. of Medical Radiology, Petersgraben 4, CH-4031 Basel, Switzerland. E-mail: klaus.scheffler@unibas.ch

Received 14 May 2002; revised 29 August 2002; accepted 8 September 2002.

DOI 10.1002/mrm.10351

Published online in Wiley InterScience (www.interscience.wiley.com).

© 2003 Wiley-Liss, Inc.

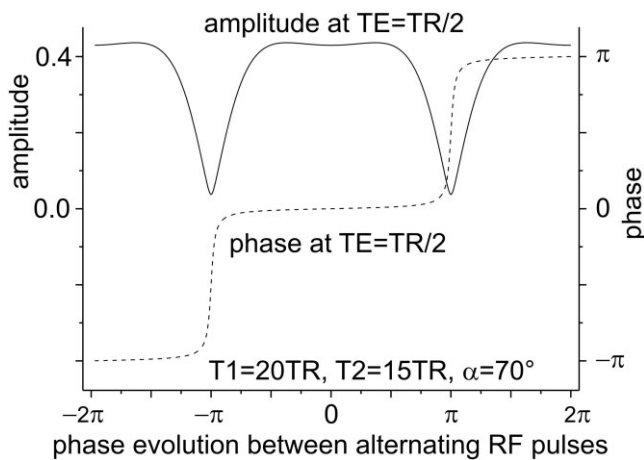


FIG. 1. TrueFISP amplitude and phase response profile calculated at $TE = TR/2$ as a function of the phase evolution between alternating excitation pulses. The magnetization is nearly refocused (approximately zero phase) at $TE = TR/2$ for dephasing angles between about $\pm 0.8\pi$.

ble to an SE or CPMG experiment wherein a complete refocusing occurs at $TE = RF\text{-spacing}/2$. The corresponding signal amplitude $M_T(TE)$ (simulated and measured) as a function of $TE = 0 \dots TR$ is depicted in Fig. 2b. Measurements were performed at 1.5T on a water sphere (10 cm diameter) using a train of alternating 70° excitation pulses ($TR = 3.6$ ms) without using any additional gradients. The acquisition window within the excitation pulses was between $0.29 TR$ and $0.69 TR$. Before acquisition the shim was optimized to 6.5 Hz, and an additional, constant gradient with 0.07 mT/m along the z-axis was applied to generate a defined distribution of frequencies (± 150 Hz) within the sphere. For the simulation the distribution of dephasing angles $p(\theta)$ was set to $\sqrt{(1.1\pi)^2 - \theta^2}$ (weighting function of the sphere) for $\theta = -1.1\pi \dots 1.1\pi$, and zero elsewhere, in accordance with the experimental conditions. Depending on the relaxation times, the simulated and measured signal intensities $M_T(TE)$ show a maximum between $TE = 0.41 TR$ and $TE = 0.49 TR$. For the chosen parameters the signal variation between $TE = 0$ and $TE = TR$ is about 30%. Some differences between simulation

and experiment can be seen for short relaxation times. This might be explained by the fact that for the simulations, excitation pulses were approximated by a single rotation at a certain time point, in contrast to the finite duration of experimental RF pulses (0.5 ms).

TrueFISP ($TR/TE = 3.6/1.8$ ms) and FLASH ($TR/TE = 3.4/1.7$ ms) images of a sphere filled with oil (top) and water are shown in Fig. 3. For Fig. 3a the scanner frequency was adjusted between the water and oil resonance, resulting in a dephasing of approximately -0.8π for oil and 0.8π for water between excitation pulses. Both resonances are thus coherently refocused at $TE = TR/2$, and no signal cancellation is visible at the oil–water interface. Setting the scanner frequency to the water resonance (Fig. 3b) generates an opposed phase for oil and signal cancellation at the oil–water interface. For the FLASH image (Fig. 3c) with $TE = 1.7$ ms, the dephasing between water and oil is about 0.75π (at $1.5T$). This gives a signal reduction at the oil–water interface that does not depend on the scanner frequency.

DISCUSSION AND CONCLUSIONS

A T_2^* -related signal decay as observed in GRE sequences is partially refocused in TrueFISP sequences. If the range of different frequencies within an imaging voxel is below $\pm 1/(2TR)$, a complete refocusing can be observed at $TE = TR/2$ for $T_1, T_2 > TR$. For shorter relaxation times, the point of refocusing is slightly before $TR/2$ and additionally shows a loss of phase coherence. The echo formation in TrueFISP is thus very similar to the CPMG technique. For both methods, dephasing effects are refocused by the excitation pulses, which leads to an echo formation at $TE = TR/2$. As can be seen from the amplitude and phase response profile of TrueFISP in Fig. 1, this refocusing mechanism fails if the dephasing between excitation pulses is more than $\pm\pi$ within an imaging voxel. For most applications, however, the field homogeneity is much better ($\pm\pi$ across the entire field of view for banding free imaging). The TrueFISP echo is nearly refocused at $TE = TR/2$ and shows an increasing T_2^* sensitivity for longer or shorter TEs. In principle, it is thus wrong and not beneficial to reduce TE in order to reduce the T_2^* sensitivity, which is

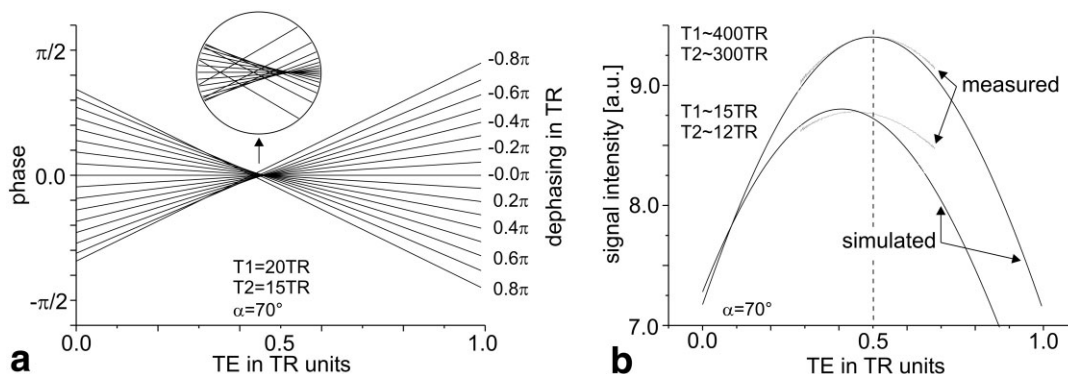


FIG. 2. **a**: Steady-state phase evolution between excitation pulses ($TE = 0 \dots TR$). For the chosen parameters the magnetization is refocused slightly before $TR/2$ and forms a spin echo. **b**: Simulated and measured transverse magnetization as a function of TE. The range of frequencies within the sphere was adjusted to ± 150 Hz, corresponding to a dephasing of about $\pm\pi$ within TR (see text).

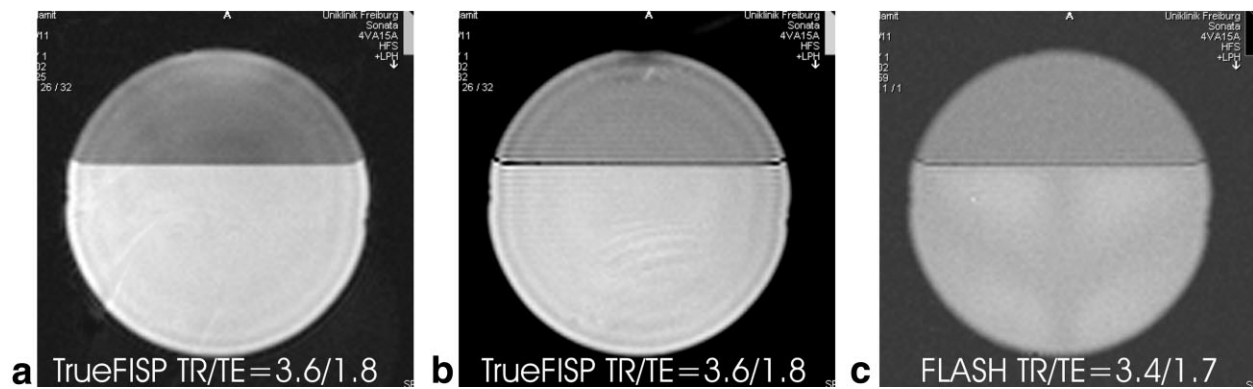


FIG. 3. TrueFISP and FLASH (balanced phase-encoding gradients, nonbalanced read and slice gradients, no RF spoiling) images of a sphere filled with water and oil (top). The magnetization of oil and water is (a) in phase (0°) if the scanner frequency is adjusted at the mean value of both resonances, and (b) in opposed phase (180°) if the scanner frequency is adjusted to the water resonance. For FLASH, the phase between oil and water is about 135° at $TE = 1.7$ ms (1.5 T), resulting in partial signal cancellation at the water–oil interface.

commonly done in FLASH sequences, and which has also been proposed for TrueFISP (4). Furthermore, the acquisition of several echoes within one TR (5–7) results in a different phase and susceptibility weighting for each echo, which again is comparable to the CPMB-based GRE and SE (GRASE) technique (8). For most applications with TR of 3–5 ms, the described T_2^* dependence is not really of practical relevance; however, it may be important in applications with long TR (9, 10).

REFERENCES

- Oppelt A, Graumann R, Barfuß H, Fischer H, Hartl W, Schajor W. FISP: eine neue schnelle Pulssequenz für die Kernspintomographie. *Electro-medica* 1986;54:15–18.
- Sekihara K. Steady-state magnetizations in rapid NMR imaging using small flip angles and short repetition intervals. *IEEE Trans Med Imaging* 1987;MI6:157–164.
- Freeman R, Hill HDW. Phase and intensity anomalies in Fourier transform NMR. *J Magn Reson* 1971;4:366–383.
- Deshpande VS, Shea SM, Chung YC, McCarthy RM, Finn JP, Li D. Breath-hold three-dimensional true-FISP imaging of coronary arteries using asymmetric sampling. *J Magn Reson Imaging* 2002;15:473–478.
- Heid O, Deimling M. Multi echo true FISP imaging. In: *Proceedings of the 3rd Annual Meeting of ISMRM, Nice, France, 1995*. p 481.
- Herzka DA, Kellman P, Aletras AH, Guttman MA, McVeigh ER. Multi-shot EPI-SSFP in the heart. *Magn Reson Med* 2002;47:655–664.
- Larson AC, Simonetti OP. Real-time cardiac cine imaging with SPIDER: steady-state projection imaging with dynamic echo-train readout. *Magn Reson Med* 2001;46:1059–1066.
- Oshio K, Feinberg DA. GRASE (gradient- and spin-echo) imaging: a novel fast MRI technique. *Magn Reson Med* 1991;20:344–349.
- Scheffler K, Seifritz E, Bilecen D, Venkatesan R, Hennig J, Deimling M, Haacke EM. Detection of BOLD changes by means of frequency-sensitive TrueFISP technique: preliminary results. *NMR Biomed* 2001;14:1–7.
- Speck O, Scheffler K, Hennig J. Fast 31P chemical shift imaging using SSFP methods. *Magn Reson Med* 2002;48:633–639.